

Dynamic Electro-Thermal Li-ion Battery Model for Control Algorithms

Original

Dynamic Electro-Thermal Li-ion Battery Model for Control Algorithms / Rizzello, A., Scavuzzo, S., Ferraris, A., Airale, A.G., Carello, M.. - ELETTRONICO. - (2020), pp. 1-6. (12th AEIT International Annual Conference, AEIT 2020 ita 2020) [10.23919/AEIT50178.2020.9241107].

Availability:

This version is available at: 11583/2910412 since: 2021-07-01T09:56:16Z

Publisher:

Institute of Electrical and Electronics Engineers Inc.

Published

DOI:10.23919/AEIT50178.2020.9241107

Terms of use:

This article is made available under terms and conditions as specified in the corresponding bibliographic description in the repository

Publisher copyright

(Article begins on next page)

Dynamic Electro-Thermal Li-ion Battery Model for Control Algorithms

Alessandro Rizzello
DIMEAS
Politecnico di Torino
Torino, Italy
alessandro.rizzello@polito.it

Andrea Giancarlo Airale
DIMEAS
Politecnico di Torino
Torino, Italy
andrea.airale@polito.it

Santo Scavuzzo
DIMEAS
Politecnico di Torino
Torino, Italy
santo.scavuzzo@polito.it

Massimiliana Carello
DIMEAS
Politecnico di Torino
Torino, Italy
massimiliana.carello@polito.it

Alessandro Ferraris
DIMEAS
Politecnico di Torino
Torino, Italy
alessandro.ferraris@polito.it

Abstract—This paper presents a fast and effective approach to evaluate the heat generation of a Li-ion battery system. The thermal characterization of Li-ion batteries is a relevant topic for the correct monitoring of the battery pack. In particular, a reduced-order model, that estimates the thermal dynamics of a Li-ion battery cell, is reported. The proposed approach relies on the definition of a boundary-value problem for heat conduction, in the form of a linear partial differential equation with the integration of Equivalent Circuit Model. The model is based on the double polarization Thévenin equivalent circuit model since it represents an optimal trade-off between accuracy and computation effort, which justifies its implementation in a Battery Management System (BMS) for automotive real-time monitoring and control. The resulting model predicts the temperature dynamics at the external surface in relation with the rate of the internal heat generation. In this paper, the model is applied to estimate the temperature of a cylindrical cell during a discharging transient and it uses electrical data acquired from experimental tests and is validated Computational fluid dynamics simulation. The results

of the test are suitable for the future implementation of a proper algorithm for State of Charge SOC and State of Health SOH estimations.

Keywords—*lithium-ion battery, battery model, Electrical Equivalent Circuit (EEC), Dual-Polarization (DP), electric vehicles, temperature analysis, automotive applications, Computational fluid dynamics (CFD), control*

I. INTRODUCTION

Battery manufacture has increased exponentially in recent years due to the increased demand for portable electrical devices. In addition, environmental issues, such as global warming, gas emissions, pollution and depletion of fossil fuels, are most discussed topics of our times. To solve these problems, efforts have been done towards E-Mobility and renewable sources, especially photovoltaic and wind. However, due to their intermittent nature, energy storage systems are required to guarantee reliable and stable operation.

The increasing demand for batteries has led manufacturers and researchers to focus on improving the energy density, safety, operating temperature, durability, output power, charging time and cost of battery technology.

Lithium-ion (Li-ion) batteries have emerged during the last two decades in response to this request.

High energy density (both gravimetric and volumetric), high efficiency, low self-discharge and relatively long life have been the major advantages of this technology in respect to other Battery Electrochemical Energy Storage (BEES) [1].

Hybrid electric vehicles (HEVs) [2], plug-in hybrid electric vehicles (PHEV) [3], [4] and pure electric vehicles (EVs) are the most important topic for research and development for automotive sector. In fact, manufacturers are developing and deploying vehicles with an increasing level of electric hybridization. This phenomenon is acting as a huge driving force for Li-ion battery technology, both from a scientific development and a mass production point of view. While automotive battery requirements vary depending on the specific vehicle's drivetrain power and level of hybridization, commonly desired characteristics are high energy and power density, high level of safety and reliability, and high life cycle number.

In addition to focusing on the formulation of new battery chemistry to improve these characteristics, the research implements increasingly sophisticated control and monitoring algorithms.

The ability to accurately predict the electrical and temperature dynamics of a battery is critical for designing onboard Battery Management Systems (BMS), and thermal management systems.

Electrical and thermal models vary in complexity. A model capturing only the electrical behaviour can be used to simple applications, [5]–[7] in other case there are more complex electrochemical models [8] that are highly accurate [9], but hard to be fully parameterized [10], and require large computational capacity. Equivalent circuit models are commonly used for control oriented applications because they are the right balance between accuracy and simplicity, and are suitable for BMS implementation [11].

The common thermal models are based on the resolution of energy conservation equations. In this way, it provides the evolution of the temperature distribution inside the battery [12].

The paper presents a combination between Equivalent circuit model and Thermal model to derive the thermal behaviour of the battery.

In the last part of the paper, a Computational Fluid Dynamics (CFD) simulation is used to validate the results obtained from the proposed model and verify the thermal behaviour of battery pack. A coupled

CFD-thermal analysis on an elementary module is performed. In such situation the cells are cooled by an external air flowrate and the mutual heat transfer between the cells is evaluated.

II. ELECTRICAL MODEL

The behaviour of Li-ion cell has been described from both electrical and thermal point of views, for this reason, a coupled electro-thermal model is used. Among the other literature models, the double polarization Thévenin equivalent circuit model is used to represent the electrical dynamic profile of a Li-ion cell in operation. The model is made up of a voltage source to represent the open-circuit voltage at thermochemical equilibrium condition, then a series resistance R_0 to account for the internal resistance of the cell and two parallel resistance-capacitance R_C blocks to describe the high non-linear and non-stationary behaviour of the cell. The first block accounts for the activation overpotential required to make the electrochemical reactions occur, whereas the second block represents the mass-transport overpotential due to the concentration gradient inside the cell. Electrical equivalent circuit models are more suitable than physical and empirical models for real-time applications due to their quite high accuracy and low computational cost.

The following equation has been used to evaluate the battery voltage response:

$$V(t) = OCV - V_1 e^{-t/\tau_1} - V_2 e^{-t/\tau_2} \quad (1)$$

A preliminary electrical cell characterization is required to evaluate the parameters of the equivalent circuit model and their dependency from both state of charge and temperature. Different experimental tests have been performed to increase the accuracy of the model and to tailor the results of the simulation with the actual cell behaviour. In particular: preconditioning test, relaxation test, capacity test and hybrid pulse power test are carried out for the whole electrical cell characterization. The first three tests are preparatory for the last one, from which the Thévenin model parameters are extracted through a set of consecutive current pulses and relaxation periods among the whole state of charge of the battery. Moreover, the hybrid pulse power characterization test is repeated for different temperature to establish its influence on the parameters. The experimental results, provided by a previous work [11], are stored inside two-dimensional lookup tables. The model's parameters have been calculated from characterization tests performed on an LG INR18650HG2 which is a Li-NMC cylindrical cell whose technical specifications are reported in Table 1. The state of charge and temperature of the cell represent the input for the lookup table, whereas the value of all the circuit parameters are the output.

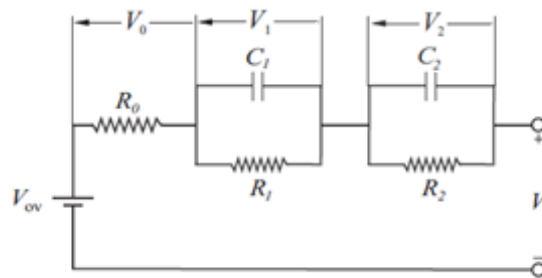


Fig. 1 2nd order Thévenin equivalent circuit

TABLE I. LG BATTERY CHARACTERISTICS

Property	Value
Nominal capacity	3.0 Ah
Nominal voltage	3.6 V
Max. voltage	4.2 V

Property	Value
Min. voltage	2.5 V
Max. discharge current	20 A
Max. charge current	4 A
Operating temperature	-20 °C to +75 °C
Cycle life	300 cycles
Diameter	18.3 mm
Height	65.0 mm

III. THERMAL MODEL

The thermal model is based on the energy conservation equation, the resolution of which provides the evolution of the temperature distribution inside the battery. The cell is treated as a solid, homogeneous and anisotropic material, thus only conductive heat transfer occurs inside the cell. The cylindrical geometry justifies the assumption of axisymmetric, thus the problem becomes two-dimensional in the radial and axial coordinates, respectively. Moreover, thermophysical properties are considered constant and temperature independent, but the anisotropy condition provides different values of thermal conductivity in the two coordinates. According to the aforementioned assumption, the governing equation of the problem becomes:

$$\rho c_p \frac{\partial T}{\partial t} = k_r \left(\frac{\partial^2 T}{\partial r^2} + \frac{1}{r} \frac{\partial T}{\partial r} \right) + k_z \left(\frac{\partial^2 T}{\partial z^2} \right) + q \quad (2)$$

where: ρ is the battery density, c_p is the specific heat capacity, k_r is the thermal conductivity in the radial direction, and k_z is the thermal conductivity in the axial direction.

The heat source rate q is made up of four terms: 1st accounts for the irreversible heat produced by the Joule effect of current flowing inside a resistive medium, the 2nd term is the reversible heat linked to the entropy variation of the electrochemical reactions, the 3rd represents the heat produced when a phase change process occurs, the 4th term is the mixing heat due to species concentration gradient inside the cell[13].

$$q = I(V_{ov} - V) - IT \frac{\partial V_{ov}}{\partial T} - \sum_i \Delta H_i^{avg} r_i - \int \sum_j (\bar{H}_j - \bar{H}_j^{avg}) \frac{\partial c_j}{\partial t} dv \quad (3)$$

where: I is the current, V_{ov} is the open-circuit voltage, V is the cell voltage, T is the cell temperature, ΔH_i^{avg} is the enthalpy variation of the chemical reaction i , r_i is the reaction rate, \bar{H}_j is the molar enthalpy of the species j , and c_j is the concentration of the species j .

In this model, the heat produced by phase change and mixing phenomena are neglected for two reasons: the lower contribution to the total heat generation rate and the complexity to evaluate experimentally these quantities. The heat source term is uniform throughout the solid domain, but it changes with time. To solve numerically the equation (2), it is necessary to adopt a proper discretization technique.

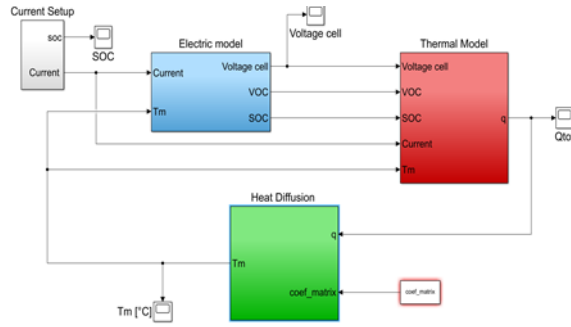


Fig. 2 Matlab-Simulink model

In this paper, a finite difference discretization approach is used to solve the heat diffusion problem in Matlab-Simulink environment. In particular:

$$\rho c_p \frac{T_{i,j}^{n+1} - T_{i,j}^n}{\Delta t} = k_r \left[\frac{1}{r_{i,j}} \left(\frac{T_{i+1,j}^{n+1} - T_{i-1,j}^{n+1}}{2\Delta r} \right) + \frac{T_{i+1,j}^{n+1} - 2T_{i,j}^{n+1} + T_{i-1,j}^{n+1}}{\Delta r^2} \right] + k_z \left[\frac{T_{i,j+1}^{n+1} - 2T_{i,j}^{n+1} + T_{i,j-1}^{n+1}}{\Delta z^2} \right] + q \quad (4)$$

The equation (4) can be written in matrix form:

$$A \times T^{n+1} = T^n + q^{n+1} \quad (5)$$

Where: A is the coefficient matrix, T^{n+1} is the unknown temperature vector at the next time step, T^n is the known vector of the temperature field at the previous time step, and q^{n+1} is the known vector of the internal heat generation rate. To solve the problem suitable boundary conditions are required, the null heat flux condition is set at the axial coordinate due to symmetry condition, whereas the conductive heat flux is imposed to be equal to the convective heat flux with external air for the outer surfaces. A transient thermal problem requires an initial value condition, the thermal equilibrium between external air temperature and cell temperature is imposed for this scope.

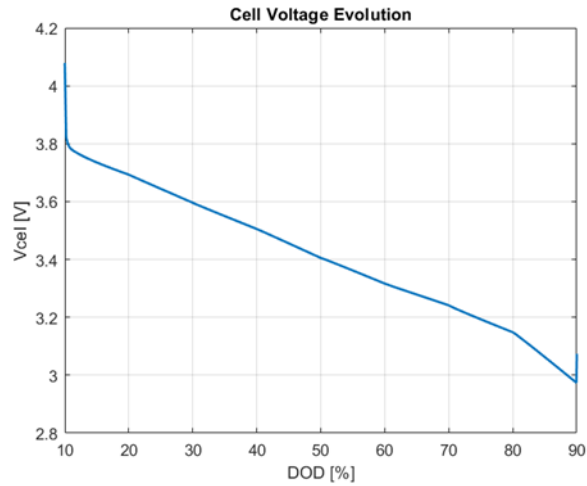


Fig. 3 Cell voltage evolution

IV. COUPLED ELECTRO-THERMAL MODEL

The presented models are linked together since the Thévenin model parameters are a function of the cell temperature, while the heat source term depends on both the open-circuit voltage and the operative voltage of the cell. Therefore, a coupled thermoelectric model is required to capture the dependency of the performance of a Li-ion battery from both electrical and thermal parameters. The model proposed (Figure 2) is developed in Matlab-Simulink environment and it simulates the discharge phase of a Li-ion battery with a current equal to its nominal capacity. The model is made up of four blocks, the current

setup block evaluates the state of charge of the cell during the whole discharging process through the Coulomb Counter algorithm. The electric model block calculates the electrical equivalent circuit model parameters through two-dimensional lookup tables function of SOC and temperature. Besides, the block solves the Kirchhoff's law to obtain the cell voltage. The thermal model block provides both the irreversible heat generation rate according to the prescribed open-circuit voltage and cell voltage, and the reversible heat generation rate as the derivative of the open-circuit voltage with respect to cell temperature lookup table. Finally, the heat diffusion block solves the energy conservation equation through finite differences discretization algorithm, and it provides the average cell temperature input for the electric model and thermal model lookup tables. The model is very powerful because it requires only few inlet parameters, the discharge current, coolant temperature and thermophysical properties of the cell such as density, thermal conductivity and specific heat capacity, but it provides as output the cell state of charge, the voltage of the cell, the internal heat generation rate and the thermal field inside the cell during the whole transient discharging process.

V. RESULTS

The model simulates the discharging phase of a li-ion cell with a constant current equal to its nominal capacity, but it could be able to simulate whatever current profile if the proper Thévenin electrical parameters are provided in the electric model block. The user can set manually some parameters of the model, in this case, the SOC limits for the discharging phase are fixed to be equal to 90% and 10% for the starting point and the ending point, respectively. The Coulomb counter algorithm is used for SOC estimation integrating the discharging current over each time step of the whole discharging process; thus, SOC evolution presents a linear trend since the applied current is constant. Figure 3 provides the cell voltage response that follows the typical polarization curve of a constant current discharging phase. Both reversible and irreversible contributions to the total internal heat generation rate are calculated. The Joule's heat source has a quite flat trend during the whole process, whereas the entropic heat source presents peaks and troughs. The highest value of the total heat generation rate occurs at the end of the process since a low state of charge provides an increase of the cell resistance. Figure 5 shows maximum, minimum and mean cell temperature evolution. The cell increases its temperature by 11°C during the discharge process. Finally, the cell temperature distribution in both radial and axial dimensions at the end of the transient is presented in Figure 6. The temperature variation along the axial coordinate is negligible thanks to the high value of thermal conductivity, the opposite trend is visible for the radial coordinate along which a thermal gradient higher than 1.7°C occurs.

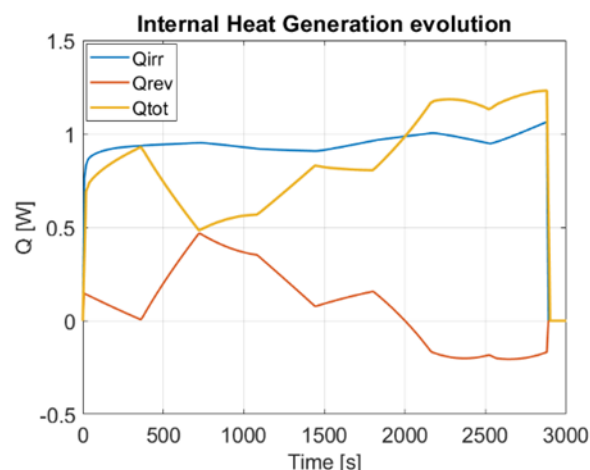


Fig. 4 Internal heat generation rate

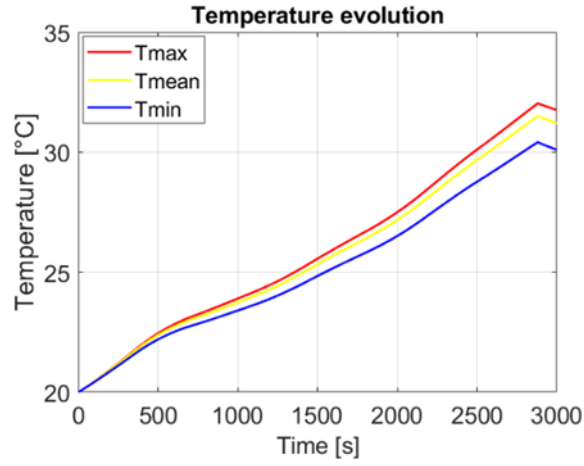


Fig. 5 Cell temperature evolution

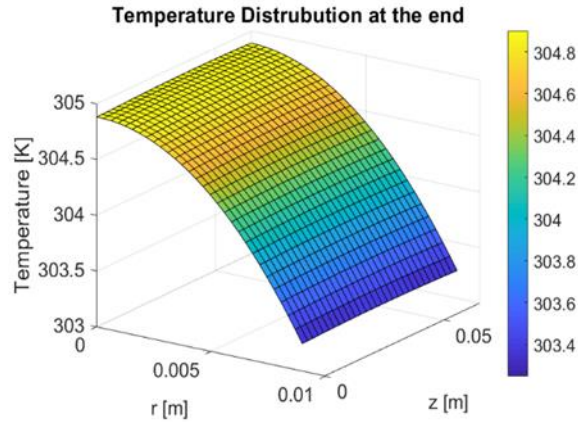


Fig. 6 Cell temperature distribution

VI. VALIDATION

A commercial software Comsol Multiphysics is used to validate the results obtained from the proposed Matlab-Simulink model. A coupled CFD-thermal analysis [14] is performed on an elementary unit made up of 9 cells, which are mechanically held by the lower and upper support. The cells are arranged with an inline configuration and both the transversal pitch and longitudinal pitch is equal to 3 mm. The lateral faces of the elementary unit represent the case of the battery pack, whereas the front and rear faces are kept open for the inlet and outlet of an external air flowrate. The heat removed by the cooling medium and the mutual heat transfer between the central cell and the surrounding cells is evaluated in the simulation. At this scope a conjugate heat transfer problem is solved, where both conductive and convective heat transfer occurs, while fluid flow is treated as laminar and incompressible.

The physic of the problem is described by mass, momentum and energy conservation laws. In the respective fluid domain, the Equations are respectively:

$$\rho \nabla \cdot (\mathbf{u}) = 0 \quad (6)$$

$$\rho (\mathbf{u} \cdot \nabla) \mathbf{u} = \nabla \cdot [-p \mathbf{I} + \mu (\nabla \mathbf{u} + (\nabla \mathbf{u})^T)] + \mathbf{F} \quad (7)$$

$$\rho c_p \frac{\partial T}{\partial t} + \rho c_p \mathbf{u} \cdot \nabla T + \nabla \cdot (-k \nabla T) = 0 \quad (8)$$

where: ρ is the air density, u is the velocity vector, p is the pressure, μ is the dynamic viscosity, F is the body force. vector, c_p is the air specific heat capacity and k is the air thermal conductivity.

In the Solid domain the equation is:

$$\rho c_p \frac{\partial T}{\partial t} + \nabla \cdot (-k \nabla T) = Q \quad (9)$$

where: ρ is the cell density, c_p is the cell specific heat capacity, k is the cell thermal conductivity and Q is the heat source.

For the fluid flow problem inlet air velocity is set to 0.1 m/s and no slip condition is imposed as boundary condition at cell-fluid interface. For the thermal problem initial temperature is fixed at 20 °C and internal heat generation source is taken as input from Matlab-Simulink model.

The results are compared with the average temperature evolution of the cell obtained from the Matlab-Simulink model. A circular optimized procedure is used, firstly the Matlab-Simulink model provides the internal heat generation rate to be used in Comsol simulations. In the CFD elementary unit simulation, the convective heat transfer coefficient is extracted from the Newton's cooling law and it is used in a second run of the Matlab-Simulink model. In particular:

$$h = \frac{-k \left(\frac{\partial T}{\partial x} \right) \Big|_{x=\text{wall}}}{(T_w - T_\infty)} \quad (10)$$

where: k is the thermal conductivity of the fluid, T_w is the surface temperature of the cell and T_∞ is the bulk air temperature. Figure 7 provides the fluid flow inside the elementary unit, from mass and momentum conservation law, fluid velocity increase when the cross section decreases, enhancing the heat removal effectiveness.

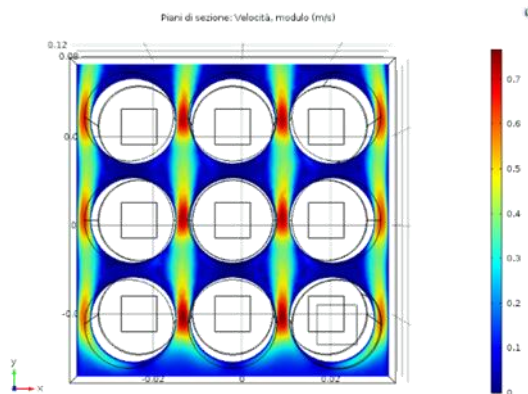


Fig. 7 Elementary unit flow field

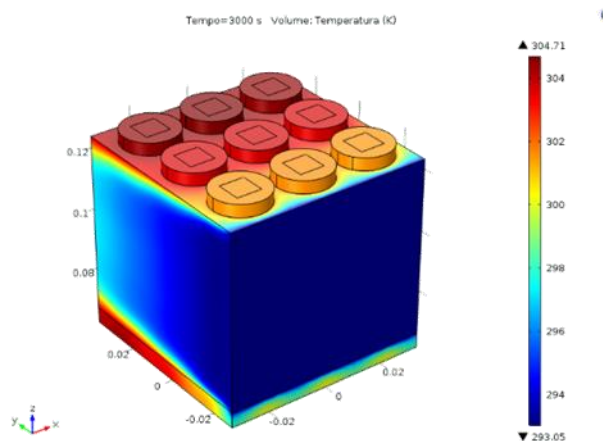


Fig. 8 Elementary unit temperature distribution

Temperature distribution inside the elementary unit is represented in Figure 8, the upper holder is removed from the picture to give an insight of the module thermal field generated by the increase of fluid temperature in the inflow direction.

Figure 10 shows high accuracy between the average temperature evolution obtained from the Matlab-Simulink simulation and the temperature evolution of the central cell of the elementary unit in the CFD simulation, a maximum error equal to 1.82% has been obtained.

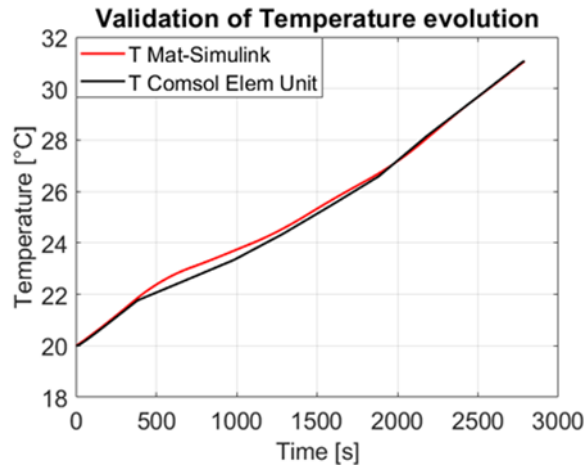


Fig. 9 Comparison of temperature evolution

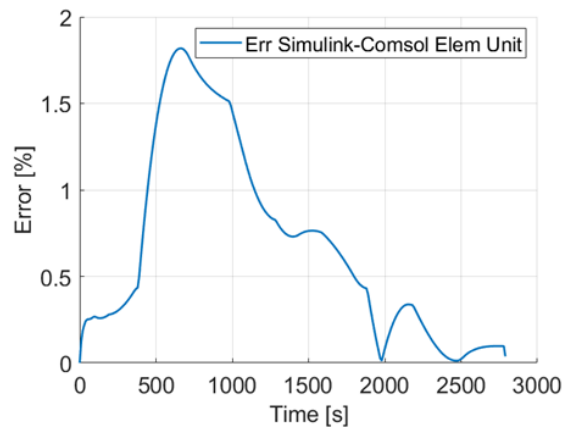


Fig. 10 Error evolution

VII. CONCLUSIONS

In this study, the numerical investigation has been carried out on both electrical and thermal transient behavior of Li-ion battery during its 1C discharge phase. A light and accurate model developed in Matlab-Simulink environment is proposed at this scope. Starting from the HPPC a complete electrical characterization of the cell under test is obtained in terms of Thévenin electrical equivalent circuit model parameters. The proposed model is able to evaluate the SOC, operative voltage, internal heat generation rate, and temperature distribution during the cell transient evolution. The following conclusions can be drawn:

- The irreversible heat source term caused by the Joule effect has a quite flat trend during the whole discharging process. This term is proportional to the cell internal resistance, which decreases when temperature increases. Nevertheless, for low values of the state of charge, electrochemical reaction rates become lower and lower due to an increase of the cell internal resistance. These two effects are counterbalanced leading to an almost constant value of the irreversible heat generation rate.

- The reversible heat source presents peaks and troughs according to the derivative of the open circuit voltage with respect to temperature behaviour.
- The total heat generation rate is given by the difference between these two terms. It presents a quite low value at high level of SOC and reaches a peak at the end of the discharge phase with a maximum value equal to 1.2 W.
- Air cooling is an ineffective thermal management system strategy; indeed, cell temperature increases monotonically during the discharge phase. At the end of the transient process cell temperature is increased by 11 °C.
- The proposed model provides the temperature distribution inside the cell and not only surface temperature. Temperature is almost constant in the axial coordinate, whereas thermal gradient occurs along the radial coordinate.
- The results obtained by the Matlab-Simulink model are validated by the CFD analysis developed in Comsol Multiphysics. Indeed, an error lower than 1.82% occurs between the temperature evolution obtained by the Simulink model and the central cell temperature evolution of the elementary unit in the CFD model.

Consequently, the proposed model is the basis for more accurate SOC estimation algorithms and SOH estimation algorithms. In addition it can be implemented in a BMS for real-time and onboard monitoring because the computational effort is low.

ACKNOWLEDGMENT

The authors want to acknowledge the Innovative Electric and Hybrid Vehicle IEHV Research group (Politecnico di Torino- DIMEAS) for providing instrumentation and facilities.

REFERENCES

- [1] M. Varini, P. E. Campana, e G. Lindbergh, «A semi-empirical, electrochemistry-based model for Li-ion battery performance prediction over lifetime», *J. Energy Storage*, vol. 25, pag. 100819, ott. 2019, doi: 10.1016/j.est.2019.100819.
- [2] M. Carello, N. Filippo, e R. d'Ippolito, «Performance Optimization for the XAM Hybrid Electric Vehicle Prototype», in *SAE Technical Paper Series*, apr. 2012, doi: 10.4271/2012-01-0773.
- [3] M. Carello, A. Airale, A. Ferraris, e A. Messana, «XAM 2.0: from Student Competition to Professional Challenge», *Comput.-Aided Des. Appl.*, vol. 11, n. sup1, pagg. S61–S67, mag. 2014, doi: 10.1080/16864360.2014.914412.
- [4] M. Carello, A. Ferraris, A. Airale, e F. Fuentes, «City Vehicle XAM 2.0: Design and Optimization of its Plug-In E-REV Powertrain», in *SAE Technical Paper Series*, apr. 2014, doi: 10.4271/2014-01-1822.
- [5] S. Scavuzzo *et al.*, «Simplified Modeling and Characterization of the Internal Impedance of Lithium-Ion Batteries for Automotive Applications», in *2019 AEIT International Conference of Electrical and Electronic Technologies for Automotive (AEIT AUTOMOTIVE)*, Torino, Italy, lug. 2019, pagg. 1–6, doi: 10.23919/EETA.2019.8804553.
- [6] E. Locorotondo *et al.*, «Electrochemical Impedance Spectroscopy of Li-Ion battery on-board the Electric Vehicles based on Fast nonparametric identification method», in *2019 IEEE International Conference on Environment and Electrical Engineering and 2019 IEEE Industrial and Commercial Power Systems Europe (EEEIC / I&CPS Europe)*, Genova, Italy, giu. 2019, pagg. 1–6, doi: 10.1109/EEEIC.2019.8783625.
- [7] E. Locorotondo *et al.*, «Modeling and simulation of Constant Phase Element for battery Electrochemical Impedance Spectroscopy», set. 2019.
- [8] T. F. Fuller, «Simulation and Optimization of the Dual Lithium Ion Insertion Cell», *J. Electrochem. Soc.*, vol. 141, n. 1, pag. 1, 1994, doi: 10.1149/1.2054684.

- [9] W. Fang, O. J. Kwon, e C.-Y. Wang, «Electrochemical-thermal modeling of automotive Li-ion batteries and experimental validation using a three-electrode cell», *Int. J. Energy Res.*, vol. 34, n. 2, pagg. 107–115, feb. 2010, doi: 10.1002/er.1652.
- [10] J. C. Forman, S. J. Moura, J. L. Stein, e H. K. Fathy, «Genetic parameter identification of the Doyle-Fuller-Newman model from experimental cycling of a LiFePO₄ battery», in *Proceedings of the 2011 American Control Conference*, San Francisco, CA, giu. 2011, pagg. 362–369, doi: 10.1109/ACC.2011.5991183.
- [11] D. Cittanti, A. Ferraris, A. Airale, S. Fiorot, S. Scavuzzo, e M. Carello, «Modeling Li-ion batteries for automotive application: A trade-off between accuracy and complexity», in *2017 International Conference of Electrical and Electronic Technologies for Automotive*, giu. 2017, pagg. 1–8, doi: 10.23919/EETA.2017.7993213.
- [12] R. Stocker, N. Lophitis, e A. Mumtaz, «Development and Verification of a Distributed Electro-Thermal Li-Ion Cell Model», in *IECON 2018 - 44th Annual Conference of the IEEE Industrial Electronics Society*, Washington, DC, ott. 2018, pagg. 2044–2049, doi: 10.1109/IECON.2018.8591633.
- [13] Y. Xiao e B. Fahimi, «Electrothermal modeling and experimental validation of a LiFePO₄ battery cell», in *2014 IEEE Transportation Electrification Conference and Expo (ITEC)*, Dearborn, MI, USA, giu. 2014, pagg. 1–5, doi: 10.1109/ITEC.2014.6861848.
- [14] R. D. Jilte e R. Kumar, «Numerical investigation on cooling performance of Li-ion battery thermal management system at high galvanostatic discharge», *Eng. Sci. Technol. Int. J.*, vol. 21, n. 5, pagg. 957–969, ott. 2018, doi: 10.1016/j.jestch.2018.07.015.